Methylparaben Isolated in Solid Argon: Structural Characterization and UV-Induced Conversion into Methylparaben Radical and Isomeric Ketenes

ARTICLE *in* THE JOURNAL OF PHYSICAL CHEMISTRY B · OCTOBER 2013

Impact Factor: 3.3 · DOI: 10.1021/jp408366x · Source: PubMed

3 AUTHORS, INCLUDING:

Rui Fausto
University of Coimbra
330 PUBLICATIONS **4,526** CITATIONS

THE JOURNAL OF PHYSICAL CHEMISTRY B

Article

pubs.acs.org/JPCB

Methylparaben Isolated in Solid Argon: Structural Characterization and UV-Induced Conversion into Methylparaben Radical and Isomeric Ketenes

Nihal Kuş,[†,‡] Sevgi H. Bayarı,[§] and Rui Fausto*[,†]

[†]Department of Chemistry, University of Coimbra, P-3004-535 Coimbra, Portugal

[‡]Department of Physics, Anadolu University, 26470 Eskişehir, Turkey

[§]Department of Physics, Hacettepe University, 06800 Ankara, Turkey

Supporting Information

ABSTRACT: Methylparaben (methyl *p*-hydroxybenzoic acid; MP) is a widely used antimicrobial preservative, being the most frequently used antimicrobial preservative in cosmetics. The generalized use of MP has become controversial, with several recent reports of dangerous side effects. For example, the presence of MP in human breast tumors and its harmful effects on human skin exposed to the sunlight have been demonstrated. In spite of the important practical relevance of the compound and of the controversy about its practical use, its structural and photochemical characterization had not been undertaken hitherto. To fill this gap, in the present study, MP was isolated in solid argon (T = 15 K) and structurally characterized by a combined infrared spectroscopy/quantum chemistry approach. The potential energy surface (PES) of the molecule was investigated in detail, revealing the existence of two almost isoenergetic (ΔE^0 = 0.37 kJ mol^{-1}) *s-cis* carboxylic ester low-energy conformers, with an estimated population ratio in the gas phase at room temperature (~298 K) of ca. 0.83. The calculations also predicted the existence of two high-energy (ΔE^0 = ~50 kJ mol^{-1}) *s-trans* carboxylic ester conformers of MP. Upon isolation of the compound in an argon matrix, only the lowest energy conformer was found to survive, due to occurrence of extensive conformational cooling during matrix deposition. The infrared spectrum of this conformer was obtained and interpreted. In addition, the chemical processes resulting from *in situ* irradiation of the matrix-isolated MP with a broadband UV source (λ > 234 nm) were investigated, revealing extensive conversion of MP into highly reactive methylparaben radical and isomeric ketenes. These observations support the recent concerns regarding uses of MP, in particular when the compound has to be exposed to UV light.

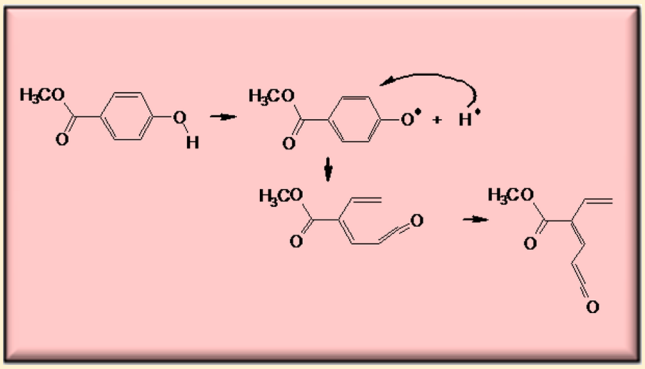

1. INTRODUCTION

Methylparaben (methyl *p*-hydroxybenzoate; MP) is a widely used antimicrobial preservative in cosmetics, food products, and pharmaceutical formulations.[1−3] It has been considered to meet most of the criteria of an ideal preservative: broad spectrum of antimicrobial activity, safe to use (i.e., relatively non-irritating, non-sensitizing, and of low toxicity), stable over a wide pH range, colorless, odorless (slight burnt flavor), non-volatile, sufficiently soluble in water to produce the effective concentration in aqueous phase, and cheap.[1,4−7] Methyl paraben consumption by humans (in food, cosmetics, and personal care products) is estimated to be larger than 50 mg/day.[1]

Though MP has been considered to have low acute and long-term toxicity, to have no carcinogenic and mutagenic activities,[1,8−10] and to be readily and completely absorbed through the skin and from the gastrointestinal tract,[1] several studies have reported that small amounts of the compound remain unhydrolyzed in the epidermis and body tissues.[11−13] For example, the presence of MP in human breast tumors has been recently reported,[14,15] and its harmful effects on human skin exposed to the sun's UV light have been demonstrated.[16−18] Such observations questioned the generalized use of MP.

In spite of the practical relevance of the compound, its structural and photochemical characterization had not been undertaken hitherto. In fact, most of the studies on MP have been centered on development of different approaches for its quantitative determination (using chromatographic or spectrometric techniques)[19−28] or evaluation of its biological effects.[1,29−31] Since MP also has adequate properties to act as a nonlinear optical material (the simultaneous presence in the

Received: August 21, 2013
Revised: October 1, 2013
Published: October 1, 2013

molecule of electron charge donor and acceptor groups provides the ground state charge asymmetry in the molecule that is required for second-order nonlinearity)[32,33] and the compound was shown to exhibit polymorphism (with at least six different polymorphs described),[34,35] several studies have also been reported which focused on the properties of the crystalline phases of MP.[32−38] However, to the best of our knowledge, no previous studies, either experimental or theoretical, were reported which focus on the isolated molecule of the compound.

In order to fill this gap, in the present study, MP was isolated in solid argon (T = 15 K) and structurally characterized by a combined infrared spectroscopy/quantum chemistry approach. First, the potential energy surface (PES) of the molecule was investigated in detail theoretically, with the purpose of determining the conformational preferences of the molecule of MP and characterizing the PES aspects related with possible conformational isomerization processes. Then, the compound was isolated in a cryogenic argon matrix, and the trapped conformational species characterized structurally by analysis of the experimental infrared spectrum and its comparison with theoretically obtained vibrational data. As it will be shown in detail in the next sections of this paper, only the lowest energy conformer was found to be present in the cryogenic matrix, due to occurrence of extensive conformational cooling[39−42] during matrix deposition. The infrared spectrum of this conformer was obtained and interpreted with the help of normal coordinates analysis. Finally, the chemical processes resulting from *in situ* irradiation of the matrix-isolated MP with a broadband UV source (λ > 234 nm) were investigated.

A matrix medium is a very convenient environment for photochemical studies, identification of reaction intermediates, and establishment of reaction mechanisms. First, because of the intrinsic simplicity and increased resolution of the vibrational spectra of matrix-isolated species, which results from the quenching of the rotational transitions, hot vibrations, and subtractive-combination vibrational transitions under these experimental conditions. Second, because matrix isolation opens the possibility of studying, at a laboratory time scale, otherwise short-life intermediates. In third place, because of the inherently greater simplicity of the photochemistry of a matrix-isolated molecule compared with those in gas phase or in solution, which results from the fact that secondary processes involving photoproduced fragments originally belonging to different molecules do not occur for the cage-confined matrix-isolated molecules. Finally, because the vibrational spectrum of a molecule isolated in a cryogenic inert matrix is, most times, practically identical to the pure vibrational spectra of the molecule *in vacuo*, thus allowing an easy and direct comparison of the experimental results with those obtained using the existing highly reliable theoretical methods. This possibility provides the researcher with a solid theoretical basis for interpretation of the experimental data.

As described below, the results obtained in the present study on the photochemistry of matrix-isolated MP revealed extensive conversion of the compound into highly reactive methylparaben radical and isomeric ketenes upon UV exposure. These results support the concerns regarding use of MP, in particular when the compound has to be exposed to UV light.

2. EXPERIMENTAL AND COMPUTATIONAL METHODS

2.1. Matrix Isolation FTIR and Photochemical Experiments. Methylparaben (MP) was obtained from Merck KGaA Darmstadt, Germany, purity ~99%. Matrices were prepared by codeposition of vapor of the compound and a large excess of argon (N60; supplied by Air Liquide) onto a CsI substrate kept at 15 K. The temperature was directly measured at the sample holder by a silicon diode sensor connected to a digital controller (Scientific Instruments, model 9650-1), with an accuracy of 0.1 K. MP was sublimated from a miniature thermoelectrically heatable glass furnace placed in the vacuum chamber of the cryostat (APD Cryogenics closed-cycle helium refrigerator with a DE-202A expander).

The IR spectra were recorded in the range 4000−400 cm^{-1}, with a resolution of 0.5 cm^{-1}, using a Thermo Nicolet 6700 Fourier-transform infrared (FTIR) spectrometer, equipped with a KBr beam splitter and a deuterated triglycine sulfate (DTGS) detector.

In the photochemical experiments, matrices were irradiated through the outer KBr window (λ > 225 nm) of the cryostat, using a HBO200 high-pressure Hg (Xe) lamp. A series of optical filters with different cutoff wavelengths (λ > 367, 325, 295, and 234 nm) were applied in the successive irradiations of the sample.

2.2. Theoretical Calculations. All theoretical calculations were performed using Gaussian 03,[43] at the DFT(B3LYP)/6-311++G(d,p) level of theory.[44−46] Calculated harmonic vibrational wavenumbers were uniformly scaled by 0.978, to correct them for the systematic shortcomings of the applied methodology (mainly for anharmonicity). The theoretical normal modes were analyzed by carrying out the potential energy distribution (PED) calculations, as described by Schachtschneider and Mortimer.[47] The internal symmetry coordinates used in this analysis (listed in Table S1 of the Supporting Information) were defined as recommended by Pulay et al.[48] For the purpose of modeling IR spectra, the scaled calculated frequencies together with the calculated intensities served to simulate the spectra shown in the figures by convoluting each peak with a Lorentzian function with a full width at half-maximum (fwhm) of 2 cm^{-1}. Note that the peak intensities in the simulated spectra are normalized to unity by the most intense peak so that the intensity scales are arbitrary units of relative intensity; on the other hand, the tables show the absolute calculated IR intensities (in km mol^{-1}).

3. RESULTS AND DISCUSSION

3.1. Potential Energy Landscape of Methylparaben. Methylparaben has four internal rotation axes, corresponding to rotations about the C−OH, exocyclic C−C, C−OCH_3, and O−CH_3 bonds. Detailed examination of the potential energy surface (PES) of the molecule allowed identification of four distinct conformers of MP resulting from conjugation of these internal rotational degrees of freedom (Figure 1).

The two lower energy conformers (**I** and **II** in Figure 1) are C_s symmetry forms exhibiting an *s-cis* methyl ester group (O═C—O—C dihedral equal to 0°). These two forms differ from each other in the relative orientation of the methoxycarbonyl and hydroxyl group: in the theoretically predicted most stable conformer (**I**), the O—H bond points to the same side of the C═O bond of the methoxycarbonyl ester, while in the higher energy conformer (**II**) the O—H bond points toward the C—OCH_3 fragment. The two *s-cis* carboxylic ester conformers of MP were predicted by the B3LYP/6-311++G(d,p) calculations to be almost isoenergetic, differing in energy only by 0.30 kJ mol^{-1} (0.37 kJ mol^{-1}, after correction of zero-point energy). At T = 298 K and P = 1 atm, $\Delta G^0_{(II-I)}$ was calculated to be 0.44 kJ

dx.doi.org/10.1021/jp408366x | J. Phys. Chem. B 2013, 117, 13543−13555

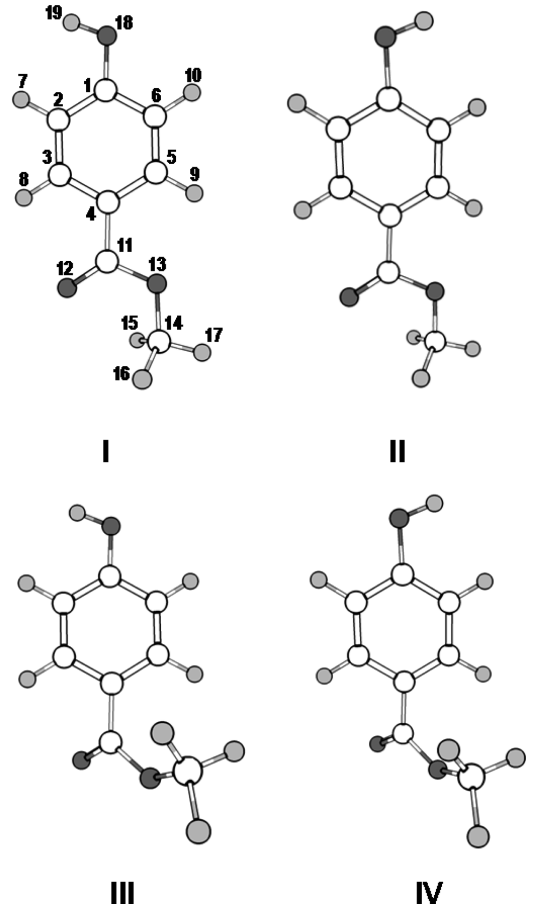

Figure 1. B3LYP/6-311++G(d,p) calculated conformers of methylparaben.

mol^{-1}, which leads to an estimation for the room temperature gas phase **II**:**I** population ratio of ca. 0.83.

The two additional conformers of MP, **III** and **IV** (see Figure 1), are high-energy forms (ΔE, ΔE^0, and ΔG^0 = 51.3, 50.2, and 49.5 kJ mol^{-1} and 52.2, 50.9, and 50.0 kJ mol^{-1} for **III** and **IV**, respectively) bearing a nearly *s-trans* carboxylic ester group. In both conformers, the methyl ester group is placed out of the molecular plane, with O═C—O—C and O═C—C_{ring}—C_{ring} dihedrals of ca. 153 and 35°, respectively, in order to minimize the effects of the unfavorable repulsive interactions resulting from the proximity of the *s-trans* carboxylic ester group methyl hydrogen atoms and the closely located ring hydrogen atom. According to the calculated relative energies of these high-energy conformers of MP, their gas phase estimated population at room temperature is neglectable (on the whole, less than 4 × 10^{-7}%).

Conformers **I** and **II** can be interconverted either by internal rotation of the hydroxyl or methoxycarbonyl groups (i.e., by internal rotation around the C—OH or exocyclic C—C bonds). The potential energy profiles corresponding to these two possibilities are shown in Figure 2. The potential energy curves were obtained by undertaking relaxed scans of the PES with the torsions about the C—OH and exocyclic C—C bonds as driving coordinates (incremented in steps of 30°), respectively. As it can be noticed in the figure, the energy barrier for rotation of the methoxycarbonyl group (31.4 kJ mol^{-1}) is nearly twice that required for rotation of the hydroxyl group (18.3 kJ mol^{-1}; which compares well with the experimental C—OH torsional

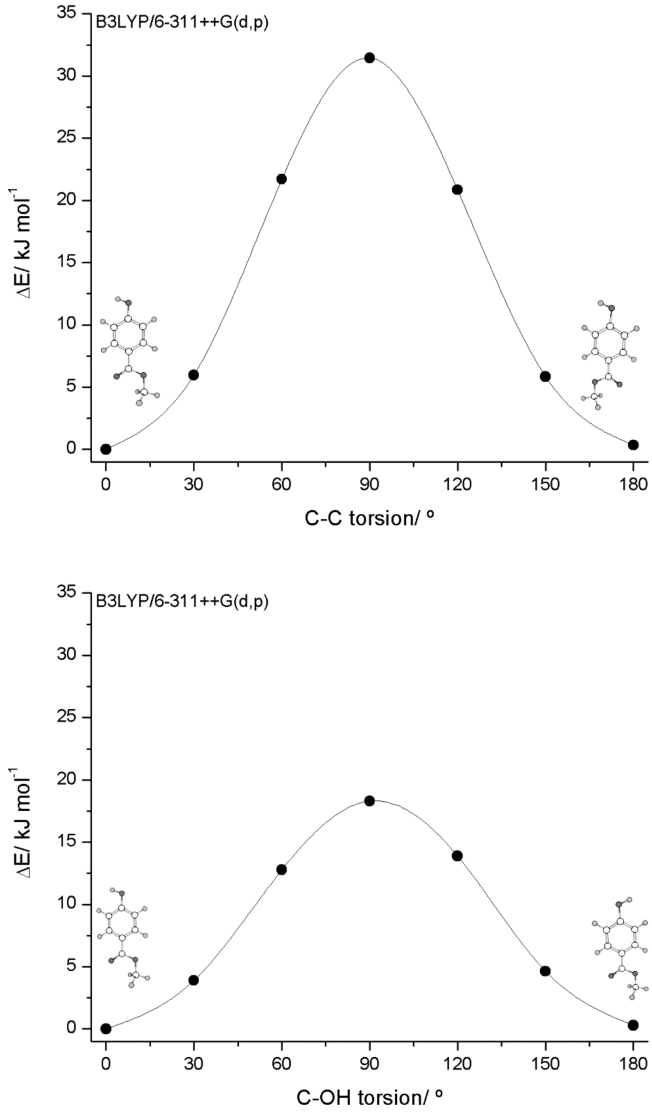

Figure 2. B3LYP/6-311++G(d,p) calculated potential energy profiles for internal rotation about the exocyclic C—C (top) and C—O (bottom) bonds in methylparaben (I → II conversion through rotation of the methoxycarbonyl and hydroxyl fragments, respectively).

barrier in phenol, 14.5 kJ mol^{-1}),[49] so that the conformational isomerization between the two low-energy forms of MP is dominated by this last process. Interestingly, the situation is quite different in the case of the isomerization between the two high-energy conformers, where the energy barrier for interconversion through rotation of the methoxycarbonyl group (7.1 kJ mol^{-1}) is smaller than that associated with the **III**—**IV** interconversion via rotation of the hydroxyl group (Figure S1; Supporting Information). This different conformational dynamics is a consequence of both the non-planarity of the high-energy conformers of MP and their high intrinsic energy. In fact, while the **III**—**IV** interconversion through rotation of the hydroxyl group is identical to the **I**—**II** interconversion and has the same associated energy barrier of 18.3 kJ mol^{-1} (this demonstrates that the conformation of the methoxycarbonyl group does not perturb the hydroxyl rotation and vice versa), the **III**—**IV** interconversion by rotation of the methoxycarbonyl group differs strongly from the corresponding one interconverting forms **I** and **II**. Keeping the OH group fixed in the plane of the ring in a given orientation, for the C_s

dx.doi.org/10.1021/jp408366x | J. Phys. Chem. B 2013, 117, 13543−13555

symmetry forms **I** and **II**, the two possible pathways for **I**−**II** interconversion are symmetry-equivalent, corresponding to a 180° rotation about the exocyclic C−C bond. On the other hand, also keeping the position of the OH group fixed, conformers **III** and **IV** correspond to two symmetry-equivalent minima on the PES each, where the methoxycarbonyl group is placed above or below the ring plane. Interconversion between the two equivalent-by-symmetry structures of each conformer implies transition through the closely located high-energy *s-trans* methoxycarbonyl C_s conformation. In turn, interconversion between **III** and **IV** keeps the methoxycarbonyl group in the same side of the ring, inplying only slight structural changes and a concerted change of 54 and 108° in the O═C—O—C and O═C—C_{ring}—C_{ring} dihedrals, respectively (see Figure S1, Supporting Information). Since the structure of the transition state for this process does not differ considerably from those of the minima, the associated energy barrier (7.1 kJ mol^{-1}) is then considerably smaller than that for the equivalent **I**−**II** interconversion (31.4 kJ mol^{-1}) and also than that for the **III**−**IV** interconversion via hydroxyl group rotation (18.3 kJ mol^{-1}).

The interconversion between the low-energy *s-cis* and high-energy *s-trans* methoxycarbonyl pairs of conformers (**I** and **III**; **II** and **IV**) occurs essentially by internal rotation about the C−OCH_3 bond. Figure S2 (Supporting Information) shows the calculated potential energy profiles corresponding to these processes resulting from relaxed scans where the torsion about this bond was chosen as a driving coordinate. As expected, the two profiles are identical, since as pointed out above the conformational dynamics of the methoxycarbonyl fragment is not influenced by the orientation of the OH group. The **III** → **I** (or **IV** → **II**) calculated energy barrier amounts only to 1.5 kJ mol^{-1} (the reverse barrier is of ∼53 kJ mol^{-1}, which is similar to the equivalent ones found, for example, in methyl formate and methyl acetate, 57.7 and 53.3 kJ mol^{-1}, respectively).[50,51] Note also that in Figure S2 (Supporting Information), for conformations corresponding to a C_{ring}—C—O—C angle smaller than ca. 90° (including for the *s-trans* methoxycarbonyl minima), the structures also have a value of the O═C—C_{ring}—C_{ring} dihedral considerably deviated from planarity. This allows the energy to be reduced by avoiding the already mentioned unfavorable repulsive interactions resulting from the proximity of the *s-trans* carboxylic ester group methyl hydrogen atoms and the closely located ring hydrogen atom. In addition, this also means that the shown potential energy profiles are not symmetric around the value 0° of the abscissas, since the transition state for interconversion between the two symmetry equivalent *s-trans* carboxylic ester forms in each plot corresponds effectively to the C_s symmetry *s-trans* carboxylic ester structure (indicated by the open circles in the figure). Decreasing the value of the driving C_{ring}—C—O—C coordinate in the performed scans to values below 0° would indeed lead to conversion between **III** and a structure located on the PES closely to conformer **IV** or between **IV** and a structure closely resembling **III** (in the scans, the constraint imposed to the value of the driving C_{ring}—C—O—C coordinate precludes, in these cases, reaching the true minima).

Finally, the potential energy profiles for rotation of the methyl group in the four conformers were also obtained. As it could be anticipated, those for the two low-energy *s-cis* methoxycarbonyl minima, **I** and **II**, were found to be identical, as well as those corresponding to the two *s-trans* methoxycarbonyl minima (**III** and **IV**). The corresponding curves are shown in Figure S3 (Supporting Information). The methyl rotation in the *s-cis* methoxycarbonyl minima has the characteristic 3-fold symmetric profile, with the stable conformations showing a C−H bond antiperiplanar to the C−O bond and an energy barrier of 3.5 kJ mol^{-1}, similar to those found in other *s-cis* methyl esters, like methyl formate (4.40−4.98 kJ mol^{-1})[50,52,53] and methyl acetate (5.05 kJ mol^{-1}).[51,54] On the other hand, in the *s-trans* methoxycarbonyl conformers **III** and **IV**, the minima along the methyl torsional potential occur for conformations where one of the C−H bonds is almost eclipsing the C−O bond (C−O−C−H dihedral equal to 17.1°). The potential exhibits a more complex form due to the simultaneous adjustments in the values of the driving coordinate and the torsions about the C−OCH_3 and exocyclic C−C bonds, and the barrier is considerably lower than that for **I** and **II** (1.7 vs 3.5 kJ mol^{-1}).

3.2. Infrared Spectrum of Matrix-Isolated Methylparaben. The analysis of the PES of methylparaben presented in the previous section allowed us to conclude that in the gas phase vapor of the compound at room temperature conformers **I** and **II** shall be populated in a **II**:**I** ratio of ∼0.83, while the high-energy forms **III** and **IV** are experimentally irrelevant under these conditions. However, the C−OH torsional energy barrier separating the two low-energy conformers of MP is small, lying in the range of values where conformational cooling during deposition of a cryogenic matrix can take place.[39−42] Conformational cooling during matrix deposition is facilitated by the circumstance that the gaseous beam being deposited carries excess thermal energy that must be dissipated during the landing of the molecules onto the cold optical substrate of the cryostat kept at 15 K. One can then expect that only the most stable conformer of MP survives to deposition of the matrix. According to the theoretical calculations, in the gas phase, this conformer corresponds to form **I**.

Figure 3 shows the infrared (IR) spectrum of a freshly deposited matrix of MP isolated in argon, at 15 K. The spectrum is compared with that obtained theoretically at the B3LYP/6-311++G(d,p) level of approximation for conformer **I**. The two spectra show a very good correspondence. However, the following observations shall be noticed: (a) the experimental spectrum exhibits extensive site spliting, due to the existence of different matrix trapping sites; this is a common feature of the spectra of aromatic molecules isolated in an argon matrix, and has been noticed, for example, in the case of matrix-isolated phenol,[55] and (b) the site-splitting is observed especially in the case of the most intense bands, so that in the calculated spectrum these bands appear comparatively most intense relative to the other, lower intensity bands; this is also a common observation, and it is easily rationalizable considering that the interactions between the isolated molecule and the matrix argon atoms are of the dispersive type, so that those vibrations giving rise to more intense IR bands, i.e., implying larger dipole moment oscillations, are also the most capable ones to induce changes in the polarizability of the matrix atoms and then change the local potential (consequently, affecting the associated vibrational frequency in a larger extension). Annealing of the matrices up to 45 K led to clearly observable site conversion, but simultaneous aggregation of the compound precluded any detailed analysis of the changes observed in the site-splitting pattern with temperature.

It shall also be pointed out that the calculated IR spectra of conformers **I** and **II** look very much identical. This fact makes it difficult to conclude, from the spectroscopic data, that only one

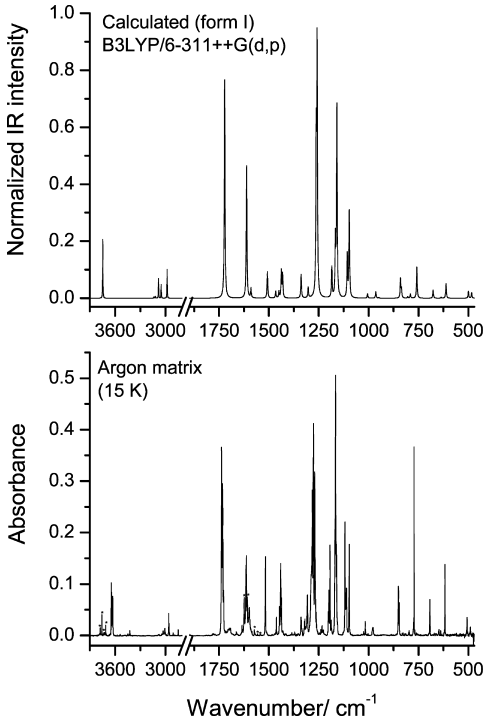

Figure 3. Infrared spectrum of methylparaben in an argon matrix at 15 K (bottom) and B3LYP/6-311++G(d,p) calculated infrared spectrum for form I. In the experimental spectrum, bands marked with asterisks represent absorptions of monomeric water present in the matrix in trace amounts. In the calculated spectrum, absorptions are represented by Lorentzian functions with fwhm = 2 cm^{-1}, centered at the calculated wavenumbers scaled by 0.978; intensities were normalized to unity.

form is present in the matrix. In fact, a simulated spectrum built from the population-weighted sum of the theoretical spectra of the two forms does also fit well the observed spectrum. However, there is experimental evidence pointing to the sole presence of one conformer (presumably form **I**) in the argon matrix. In the first place, deposition of vapor of the compound of different temperatures (from room temperature to nearly 250 °C) gives rise to exactly the same spectrum, with no changes in the relative band intensities. Taking into account the relative energy of the two forms, the increase of temperature from room temperature to ∼250 °C would produce a change in the **II**:**I** population ratio from ca. 0.83 to ∼0.92, which should in principle be noticeable. In addition, as it will be described in detail in the next section, upon UV irradiation (λ > 234 nm) of matrix-isolated MP, the bands of the compound decrease in intensity, indicating its consumption, while bands due to photoproduced species emerge. However, all MP bands were found to decrease according to the same kinetics, suggesting once again the presence of only one form in the matrix.

We have also checked for any spectral change that could indicate a conformational conversion (either change in the relative intensities of the initially present bands or appearance of new bands) by performing *in situ* narrow-band near-IR irradiations of the matrix-isolated MP at wavenumbers within the νOH stretching overtone band profile (between 7122 and 7080 cm^{-1}; see Figure S4, Supporting Information). These types of experiments have been successfully used to change the relative populations of conformers differing by internal rotation of a hydroxyl group in several molecules.[56−60] However, in the present case, no changes in the experimental spectrum were observed, even after quite prolonged irradiation in the near-IR. There are two possible explanations for this result: (i) the energy relaxation mechanism coupling the νOH stretching overtone with the hydroxyl torsion is not active in this molecule, or (ii) considering the low energy barrier for internal rotation of the hydroxyl group in MP, any putative conformational conversion taking place upon the near-IR irradiations was promptly made unobservable in the time scale of our experiments by occurrence of a fast tunneling back-reaction. The last type of situation has been found, for example, in glycine and alanine isolated in an argon matrix.[61,62] Future experiments for the compound in a cryogenic N_2 matrix (where specific interactions between the O−H group and the nitrogen matrix atoms usually stabilize different conformers)[61−64] may eventually allow for a definitive answer to this question.

The fact that the experimental spectrum of matrix-isolated MP is well reproduced theoretically allowed us to undertake a detailed assignment of the observed bands. This is presented in Table 1, together with the results of the performed normal coordinates analysis.

3.3. *In situ* UV Irradiation of Matrix-Isolated Methylparaben. As mentioned in the Introduction section, methylparaben has been found to lead to harmful effects on human skin exposed to the sun's UV light.[16−18] In addition, strategies have been proposed for photodegradation (photooxidation) of MP contaminant (and of parabens in general) in wastewater.[65−68] Nevertheless, the photochemical behavior of the compound has been scarcely characterized, and in all studies reported hitherto the presence of an active solvent or enhancers (e.g., TiO_2, H_2O_2) precluded the detailed investigation of MP intrinsic photochemistry.

In the present study, matrix-isolated methylparaben was submitted to *in situ* UV irradiation using a broadband UV source and a series of optical filters with different cutoff wavelengths (λ > 367, 325, 295, and 234 nm). The irradiations were performed consecutively using filters of decreasing cutoff wavelength. When the λ > 325 cutoff filter was used, changes in the infrared spectrum of the MP matrix started to be noticeable, indicating that the compound has begun to react. Specifically, MP bands decreased in intensity and new bands, ascribable to newly formed species, emerged in the spectrum. Though the spectral changes were found to be mostly identical when either the λ > 325, 295, or 234 nm cutoff filters were used, the photochemical processes were found to be considerably more efficient when this later filter was used. This is consistent with the UV absorption spectrum of methylparaben, which has been reported previously:[69] 325 nm corresponds to the beginning of the long wavelength wing of the absorption band, which shows its maximum near 260 nm.

The first conclusion extracted from the irradiation experiments was that all bands of MP began to decrease in intensity simultaneously and at the same rate. Such behavior strongly supports the idea that a single conformer of methylparaben was trapped in the matrix. The second observation was that more than one product was being formed, since the new bands in the spectrum follow different patterns of growing along the irradiation. Moreover, subsequent irradiation of the matrix previously irradiated using the 234 nm cutoff filter with the 325 nm filter (which has been first shown to be quite ineffective to induce the phototransformation of MP into other species) led to a selective growing of a few product bands, while the other product bands kept their intensity nearly constant. The third

dx.doi.org/10.1021/jp408366x | J. Phys. Chem. B 2013, 117, 13543−13555

Table 1. B3LYP/6-311++G(d,p) Calculated Wavenumbers (ν; cm^{-1}), Infrared Intensities (I^{IR}; km mol^{-1}), and Potential Energy Distributions (PED; %) Resulting from Normal Coordinates Analysis for Methylparaben (form I)[a]

experimental	calculated		
ν^b	ν^b	I^{IR}	PED[c]
3646/3643/3642/3638/3535/3532/3629/3627/3626	3746	84.2	ν(O—H)(100)
3093	3141	1.1	νCH ring1(46) + νCH ring2(39)
3086	3130	3.1	νCH ring2(33) + νCH ring1(31) + νCH ring3(22) + νCH ring4(13)
3079	3122	1.2	νCH ring3(46) + νCH ring4(39)
3044	3085	16.1	νCH ring4(33) + νCH ring3(32) + νCH ring2(18) + νCH ring1(17)
3030	3084	14.4	$\nu(CH_3)'_{as}$(97)
3018/3009/3005	3053	19.6	$\nu(CH_3)''_{as}$(100)
3963/3960/3956/3955	2982	41.3	$\nu(CH_3)_s$(98)
1737/1733/1732/1731/1728/1727/1725	1722	317.7	ν(C═O)(85)
1615/1613	1612	163.2	νCC ring2(62) + δCH ring1(17) + δring2(10)
1598	1590	55.3	νCC ring3(64)
1518/1517	1507	47.0	δCH ring4(52) + νCC ring5(35)
1461	1466	9.7	$\delta(CH_3)'_{as}$(81) + $\gamma(CH_3)'_{as}$(10)
1447/1444	1450	9.1	$\delta(CH_3)''_{as}$(93)
1441	1438	23.7	$\delta(CH_3)_s$(86)
1438/1437	1431	9.2	δCH ring2(40) + νCC ring6(37)
1339/1338/1337/1334/1333/1324/1321/1319	1338	11.9	νCC ring4(40) + νCC ring6(23) + δ(COH)(19) + δCH ring3(15)
1308/1396/1305	1303	22.2	δCH ring3(73) + νCC ring4(18)
1290/1288/1286/1282/1278	1263	147.1	$\nu(C_{(4)}—C_{(11)})$(24) + δCH ring4(23) + $\nu(C_{(11)}—O)$(16) + δring1(12)
1276/1271/1270/1269/1268/1267	1258	471.6	$\nu(C_{(1)}—O)$(42) + νCC ring1(22)
1202/1199/1997/1993	1184	53.4	$\gamma(CH_3)'_{as}$(72) + $\delta(CH_3)'_{as}$(10)
1169	1166	72.2	δ(COH)(50) + δCH ring2(23) + νCC ring4(14)
1166/1164/1161	1159	274.3	δCH ring1(72) + νCC ring2(16)
1157/1156	1145	0.8	$\gamma(CH_3)''_{as}$(92)
1119/1113/1112/1111/1109	1107	85.9	δCH ring2(25) + $\nu(C_{(11)}—O)$(16) + $\nu(C_{(14)}—O)$(15)
1098/1097	1097	69.8	δCH ring2(34) + νCC ring6(24)
1017/1016/1015/1014	1005	6.2	δ ring1(41) + νCC ring5(39) + δCH ring4(16)
982	966	0.1	γCH ring2(36) + τ ring3(21) + γCH ring3(19) + γCH ring1(13)
980/979/978/976	964	12.0	$\nu(C_{(14)}—O)$(66)
956	949	0.8	γCH ring4(31) + γCH ring1(27) + γ(C═O)(22) + τ ring1(14)
852/851/849/848	840	25.3	γCH ring(39) + γCH ring4(14) + γ(C═O)(11)
847/846	835	13.9	νCC ring1(41) + $\nu(C_{(1)}—O)$(12) + δ ring2(12) + $\nu(C_{(11)}—O)$(11)
817	804	2.7	γCH ring1(33) + γCH ring4(29) + γCH ring2(26)
798/797	791	6.1	δ(OCO)(24) + $\nu(C_{(11)}—O)$(14) + δ ring1(14) + $\nu(C_{(1)}—O)$(11)
772/771	758	46.0	γ(C═O)(55) + $\gamma(C_{(1)}—O)$(13) + $\gamma(C_{(4)}—C_{(11)})$(12)
694/693	677	12.4	τ ring1(37) + $\gamma(C_{(1)}—O)$(24) + γ(C═O)(14)
649/648/647/638	636	2.0	δ ring3(75) + νCC ring3(13)
618/617/616	612	19.4	δ ring2(30) + δ(OCO)(17) + $\nu(C_{(4)}—C_{(11)})$(13) + δ ring1(11) + $\nu(C_{(1)}—O)$(11)
508/506	500	10.3	$\gamma(C_{(1)}—O)$(45) + $\gamma(C_{(4)}—C_{(11)})$(21) + τ ring2(11)
490	483	0.8	δ(CCO)(38) + w$(C_{(4)}—C_{(11)})$(17) + w$(C_{(1)}—O)$(13)
n.i.	411	0.7	τ ring3(50) + τ ring2(17)
n.i.	393	19.7	w$(C_{(1)}—O)$(56) + δ(CCO)(13)
n.i.	335	106.8	τ(OH)(89)
n.i.	323	5.1	δ ring2(33) + δ(COC)(26) + $\nu(C_{(4)}—C_{(11)})$(24)
n.i.	305	9.5	δ(COC)(35) + δ(OCO)(25) + w$(C_{(4)}—C_{(11)})$(17)
n.i.	294	8.2	$\gamma(C_{(4)}—C_{(11)})$(29) + τ ring1(25) + $\tau(C_{(11)}—O)$(10) + τ(OH)(10)
n.i.	164	2.7	$\tau(C_{(11)}—O)$(46) + $\tau(CH_3)$(24) + τ ring2(16)
n.i.	144	1.1	w$(C_{(4)}—C_{(11)})$(47) + γCH ring1(31) + γCH ring2(11)
n.i.	131	0.6	$\tau(CH_3)$(73) + $\tau(C_{(11)}—O)$(13)
n.i.	85	0.5	τ ring2(29) + $\tau(C_{(11)}—O)$(22) + $\gamma(C_{(4)}—C_{(11)})$(16)
n.i.	57	0.5	$\tau(C_{(4)}—C_{(11)})$(87)

[a] ν, stretching; δ, bending; γ, rocking; w, wagging; τ, torsion; s, symmetric; as, asymmetric; n.i., not investigated. See Table S1 (Supporting Information) for the definition of the symmetry coordinates. [b] Wavenumbers were scaled by 0.978. [c] PEDs lower than 10% are not included.

observation was that one type of photoproducts contributing to the spectra registered along the irradiation experiments should bear the ketene moiety, because the very characteristic νC═C═O ketene antisymmetric stretching infrared band is present in these spectra at its usual wavenumber position (~2140–2100 cm^{-1} range).[55,70−73] Finally, an additional conclusion could be extracted from the profiles of the bands due to the product species, which are in general quite narrow, suggesting that the observed reactions should not correspond to photofragmentation reactions leading to species which could then form associates with each other within the matrix primary occupied cage. These associates can, indeed, be expected to

dx.doi.org/10.1021/jp408366x | J. Phys. Chem. B 2013, 117, 13543−13555

possess a substantial intermolecular structural flexibility, resulting in broader infrared bands.

In view of the observations described above, in particular the experimental evidence indicating formation of an isomeric ketene as one of the photoproducts of matrix-isolated MP, the photochemistry of the compound appeared to be similar to those previously reported for matrix-isolated phenol and for phenol derivative triclosan (5-chloro-2-(2,4-dichloro-phenoxy)-phenol), which have been investigated before in our laboratory.[55,73] For these last compounds, the primary photochemical step was found to be the photocleavage of the phenolic O−H bond, to form an H atom and the corresponding phenoxyl radicals.[55,73] In the case of phenol (and phenol-d_5), the formed radical could be detected and characterized spectroscopically in the cryogenic matrices.[55] The radical has been shown to convert subsequently to other products, all of them isomers of phenol, specifically 2,5-cyclohexadienone, Dewar phenol and the open-ring ketene (see Figure S5, Supporting Information). These three secondary photoproducts of matrix-isolated phenol result from recombination of the initially formed phenoxyl radical with the H atom: 2,5-cyclohexadienone from attack to the *para*-position of the aromatic ring; the Dewar and ketene species from attack to the *ortho*-position through intermediacy of 2,4-cyclohexadienone[55] (attack to the *meta*-position would lead to a high-energy bicyclopropanone species and was proved to be unfavored).

With this in view, one searched for the spectral signature of the metylparaben phenoxyl radical in the spectra of the photolyzed matrix-isolated MP. Figure 4 shows a representative region (1000−550 cm^{-1}) of the infrared spectra of the photolyzed MP matrix, together with the same region of the spectrum of the as-deposited matrix of the compound.

The same figure shows also the calculated IR spectra for methylparaben radical and the most stable conformer of MP (form **I**). It is clear from this figure that the spectrum of the radical fits well the observed bands of the photoproduct. In fact, all significantly intense bands of the methylparaben radical predicted theoretically (Table 2; see also Table S2, Supporting Information) could be observed experimentally (the exceptions are the bands due to the νC−H stretching modes, which as usual for matrix-isolated species have IR intensities much lower than those theoretically predicted for the gas phase). The observed photoproduction of methylparaben radical is in agreement with the observation of Handa et al., who found that MP is a source of radicals when irradiated with UV light, in particular of hydrogen atoms.[16]

It shall also be noticed that the spectrum of the irradiated matrix presented in Figure 4 was registered after 14 min of irradiation at λ > 234 nm + 2 h at λ > 325 nm. However, in what concerns the bands of the radical, this spectrum is practically equal to that recorded after only the 14 min of irradiation at λ > 234 nm, since the irradiation at λ > 325 nm does not affect much the intensity of the bands ascribable to this species (Figure 5). On the other hand, the bands due to the reactant (MP) were about half intense in the spectrum shown, compared to that obtained after only 14 min of irradiation at λ > 234 nm, and 1:4 as intense as in the spectrum of the non-irradiated matrix (see Figure 5). Assuming that the photochemical process is first-order, this last result indicates that the rate of the MP photoreaction reduces by a factor of ca. 8.5 by changing the cutoff filter used during the irradiation from λ > 234 nm to λ > 325 nm. In addition, it can also be concluded that, since the irradiation at λ > 325 nm kept the concentration

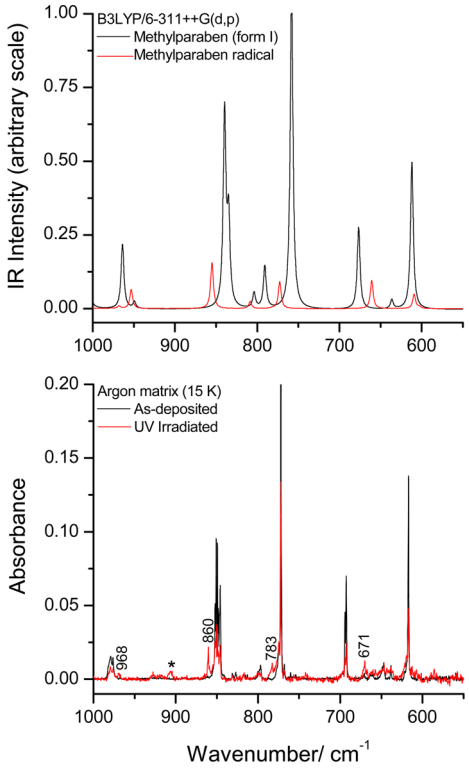

Figure 4. Bottom: 1000−550 cm^{-1} region of the IR spectra of the as-deposited argon matrix of methylparaben (black line) and of the same matrix after UV irradiation (14 min at λ > 234 nm + 2 h at λ > 325 nm; red line); the product band about 900 cm^{-1} (marked with the asterisk) belongs to the methylparaben isomeric ketene (Z form). Top: B3LYP/6-311++G(d,p) calculated IR spectra of methylparaben (black line) and methylparaben radical (red line). In the calculated spectra, bands are represented by Lorentzian functions with fwhm = 2 cm^{-1}, centered at the calculated wavenumbers scaled by 0.978 and intensities scaled by factors leading to approximate reproduction of the experimental data.

of the radical nearly constant, the rate of consumption of this species into subsequent reactions is approximately equal to that of its formation from MP upon irradiation at this wavelength. Finally, it shall also be noticed that the product band observed at 906 cm^{-1} and marked in Figure 4 with an asterisk shows a very low intensity in the spectrum obtained after irradiating the matrix at only λ > 234 nm (by 14 min). This band shall then belong to a secondary product, which will be disclosed below.

Continuing to use the previously observed photochemistry of matrix-isolated phenol[55] as a model, one searched for any evidence of the products which, in the case of MP, would be the equivalent ones of the phenol products 2,5- and 2,4-cyclohexadienones (i.e., 4-methoxycarbonyl-2,5-cyclohexanedienone, which would result from attack of the initially formed H atom to the *para*-position of the aromatic ring of MP radical, and 4-methoxycarbonyl-2,4-cyclohexanedienone, the first species to be produced as a result of attack of the H atom to the *ortho*-position of MP radical). The calculated infrared spectra for these two structural isomers of methylparaben were obtained theoretically and compared with the experimental data. It became clear that none of these two species were contributing to the spectra of the photolyzed matrix of MP. Also, we considered the possibility of formation of Dewar methylparaben isomer, but comparison of its theoretically predicted infrared spectrum with the experimental spectra

dx.doi.org/10.1021/jp408366x | J. Phys. Chem. B 2013, 117, 13543−13555

Table 2. Assignment of the Observed Bands for Methylparaben Radical (MP•)[a]

calculated[b]		observed	
ν	I^{IR}	ν	approximate description[c]
1716	262.8	1727	ν(C═O)
1558	20.4	1556	νCC ring
1469	7.1	1465	νCC ring
1456	15.9	1458	δCH ring, ν(C—O•)
1450	10.3	1447	$\nu CH_3''_{as}$
1438	26.7	1443	$\nu CH_{3\,s}$
1396	19.7	1390	δCH ring, νCC ring
1393	13.0	1387	δCH ring, νCC ring
1284	53.2	1295	νCC ring
1258	464.5	1277	ν(C—O), ν(C—C)
1186	46.4	1197	$\gamma CH_3'$
1140	81.6	1145	νCH ring
1095	61.3	1103	ν(C—C), ν(C—O)
1086	39.6	1090	δCH ring
953	16.3	968	ν(O—C(H_3))
855	39.2	860	γCH ring
773	23.0	783	γ(C═O)
661	24.0	671	τ ring

[a]Wavenumbers (ν) in cm^{-1}; infrared intensities (I^{IR}) in km mol^{-1}; ν, stretching; δ, bending; γ, rocking; τ, torsion; s, symmetric; as, asymmetric. [b]Calculated wavenumbers scaled by 0.978; see Table S2 (Supporting Information) for a full list of calculated wavenumbers and infrared intensities. [c]Approximate descriptions obtained through analysis of the animated vibrations using the Gaussview (version 3.0) program.[74]

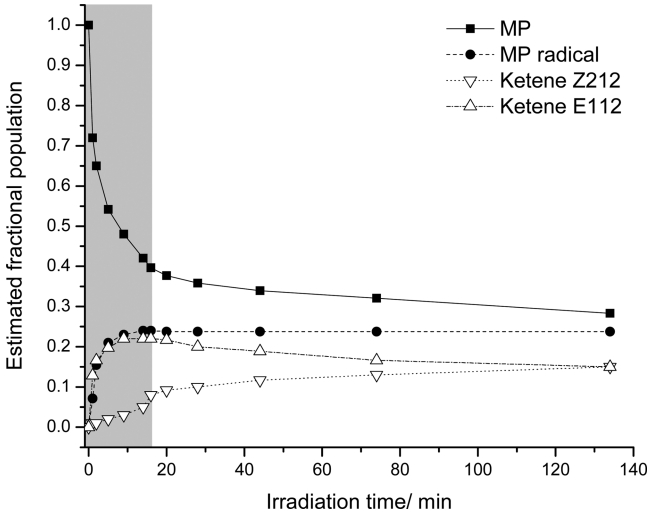

Figure 5. Estimated populations of MP, methylparaben radical, and ketene forms (Z212 and E112) along the irradiation experiments (234 and 325 nm). The populations were estimated from the change with irradiation time of the integral intensities of the bands at 1166 cm^{-1} (MP), 860 cm^{-1} (methylparaben radical), ~2127 cm^{-1} (ketene Z212), and ~2120 cm^{-1} (ketene E112). The intensities were first reduced by dividing the absorbance by the calculated intensities and then normalized by the intensity of the reactant band. The gray area corresponds to irradiations at 234 nm.

showed that such a molecule had not been formed either. Indeed, all product bands observed in the spectra of the photolyzed matrix of MP not ascribable to methylparaben radical could be assigned to ketene species isomeric of methylparaben, as described below.

The key information for identification of the ketenes was the appearance, in the ~2140−2100 cm^{-1} range of the spectra of the photolyzed matrix of MP, of the very characteristic[55,70−73] νC═C═O ketene antisymmetric stretching infrared band. Figure 6 (top panel) shows the spectra of the as-deposited MP

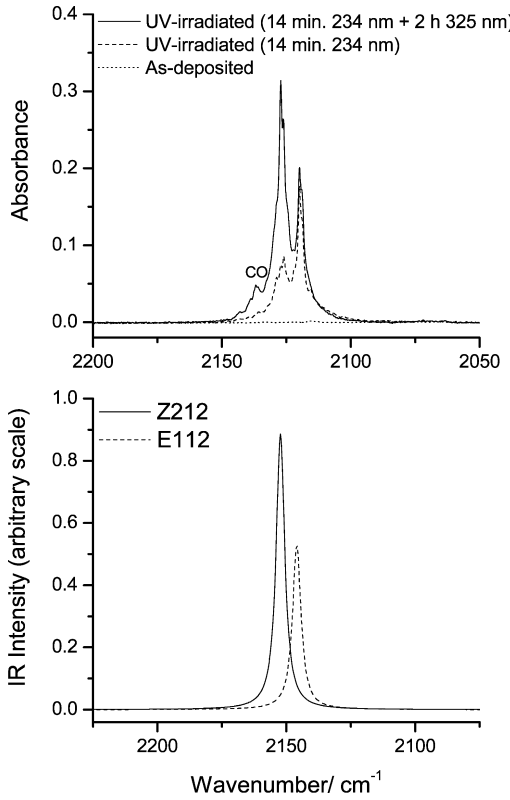

Figure 6. Top: ν(C═C═O) as. region of the IR spectra of the as-deposited argon matrix of methylparaben (dotted line) and of the same matrix after UV irradiation: 14 min at λ > 234 nm (dashed line) and 14 min at λ > 234 nm + 2 h at λ > 325 nm (solid line); the product band at about 2138 cm^{-1} belongs to carbon monoxide. Bottom: B3LYP/6-311++G(d,p) calculated ν(C═C═O) as. IR bands for methylparaben isomeric ketene: form Z212 (solid line); form E112 (dashed line); see Figure 7 for structures of the ketene forms. In the calculated spectra, bands are represented by Lorentzian functions with fwhm = 2 cm^{-1}, centered at the calculated wavenumbers scaled by 0.978 and intensities in an arbitrary scale which respects the predicted relative intensities for the two forms. Note the shift in the abscissas in the calculated spectra relatively to the experimental data.

matrix and those of the irradiated matrix (after 14 min of irradiation at λ > 234 nm and after an additional 2 h of irradiation at λ > 325 nm). It is clear from this figure that the two main absorptions, at about 2127 and 2120 cm^{-1}, behave differently along the irradiation experiments: the lower wavenumber band grows during irradiation at λ > 234 nm, keeping its intensity nearly constant during irradiation at λ > 325, while the higher wavenumber band grows mostly during the irradiation at λ > 325 nm. A similar behavior has been found before for other ketenes resulting from a ring-opening reaction of a six-membered unsaturated ring (e.g., phenol,[55] 2-pyranones),[72] where the ketene moiety is conjugated with a double bond. Such behavior was concluded to result from the isomerization of the initially produced conjugated ketene in one E/Z isomeric configuration, geometrically more similar to the

dx.doi.org/10.1021/jp408366x | J. Phys. Chem. B 2013, 117, 13543−13555

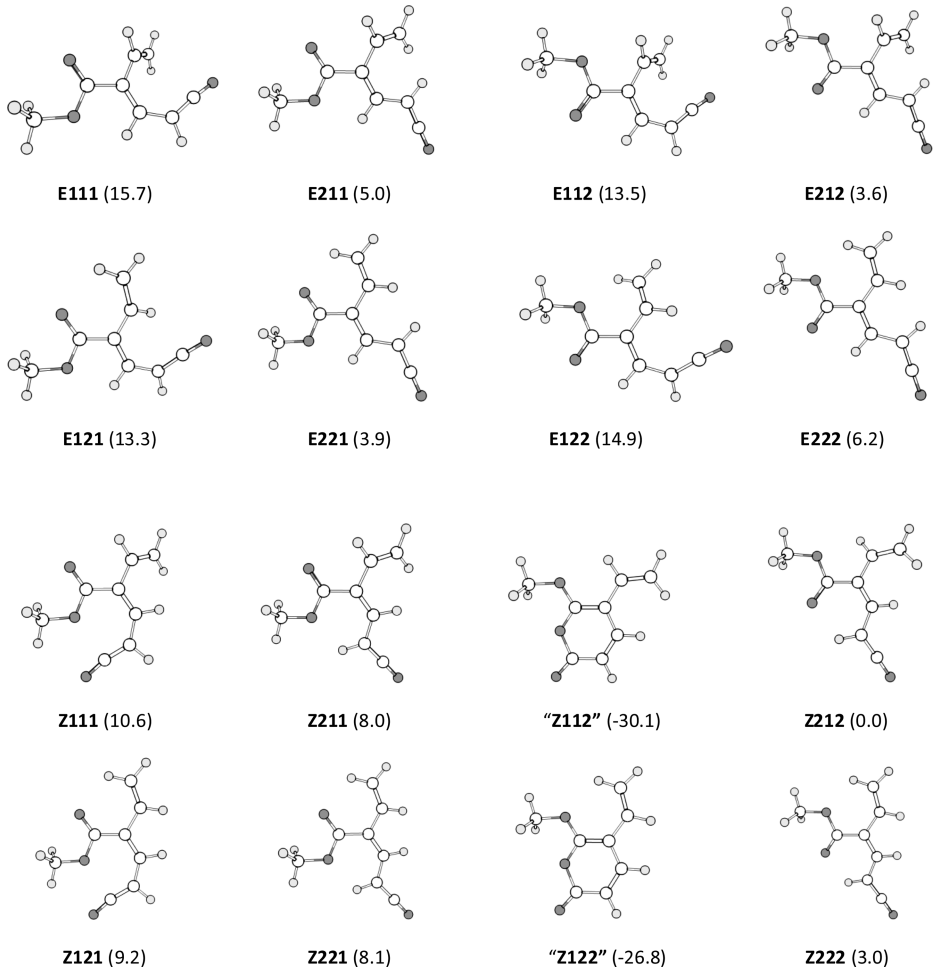

Figure 7. Conformers of the ketene isomer of methylparaben (zero-point corrected energies, in kJ mol^{-1}, in parentheses). The notation used considers four symbols: the first letter defines the configuration ("entgegen", E, or "zusammen", Z) about the central C═C bond, and the three numbers represent two possible orientations (1 or 2) of the ketene, vinyl, and methoxycarbonyl groups, respectively. Forms Z112 and Z122 are not stable, and converge to the closed-ring isomer 5-ethenyl-6-methoxy-2*H*-pyran-2-one (two different conformers of this compound).

Table 3. B3LYP/6-311++G(d,p) Calculated Wavenumbers (ν/cm^{-1}; Scaled by 0.978) and Infrared Intensities (I^{IR}/km mol^{-1}) and Experimentally Observed Bands for Methylparaben Isomeric Ketene Forms E112 and Z212[a]

E112				Z212			
calculated[b]		observed		calculated[b]		observed	
ν	I^{IR}	ν	approximate description[c]	ν	I^{IR}	ν	approximate description[c]
2146	994.3	2120/2119	νC═C═O as	2152	1670.7	2127/2126	νC═C═O as
1716	293.6	1727	νC═O	1695	213.7	1697	νC═O
1640	25.7	1642	νC═CH_2	1634	42.9	1639	νC═CH_2
1598	284.3	1594	νC═C	1579	338.2	1554/1549	νC═C
1234	644.7	1256/1254	νC—O	1309	61.8	1314	δCH
1086	35.5	1093	νC—C	1296	109.2	1298	δCH
1064	54.5	1073	wCH_2	1218	360.1	1246	νC—O
925	36.8	1000	νO—CH_3	1185	120.8	1195	$\gamma OCH_3'$
597	63.0	585	γCH (ketene)	1147	228.7	1152	δCH (ketene)
				1078	57.3	1082	νC—C
				1015	19.9	1027	γCH
				909	47.9	906	wCH_2

[a]Wavenumbers (ν) in cm^{-1}; infrared intensities (I^{IR}) in km mol^{-1}; ν, stretching; δ, bending; γ, rocking; w, wagging; as, asymmetric. [b]Calculated wavenumbers scaled by 0.978; see Table S2 (Supporting Information) for a full list of calculated wavenumbers and infrared intensities. [c]Approximate descriptions obtained through analysis of the animated vibrations using the Gaussview (version 3.0) program.[74]

closed-ring species, into the other (usually more stable) E/Z isomer. In order to explore this possibility, we calculated the structures, relative energies, and IR spectra of all possible ketene isomeric forms which can be obtained from

dx.doi.org/10.1021/jp408366x | J. Phys. Chem. B 2013, 117, 13543−13555

methylparaben by cleavage of a C−C α-bond to the hydroxyl group accompanied by [1,3]-H atom migration of the hydroxylic hydrogen atom. The results are summarized in Figure 7 and Table 3 (see also Table S2, Supporting Information). The used notation for the ketene isomers considers four symbols: the first letter defines the configuration ("entgegen", E, or "zusammen", Z) about the central C═C bond, while the three numbers represent two possible orientations (1 or 2) of the ketene, vinyl, and methoxycarbonyl groups, respectively.

According to the geometry of the reactant closed-ring species, the most probable ketene isomers formed upon the ring-opening reaction shall be of E type, whose structure resembles more that of the closed-ring precursor. This preference for products structurally resembling more the reactant species is the general rule for this type of reactions in low temperature solid matrices (principle of least motion),[75,76] since they require not just a minimal rearrangement of the reacting species itself but also a negligible rearrangement of the matrix atoms surrounding the molecule. Ketene forms E111 and E112 are, among all possible conformers of the ketene isomeric E form, those resembling more the closed-ring precursor, and, between these two, E112 has the lowest energy. On the other hand, ketene Z conformers are generally more stable than E forms, the most stable Z-type conformer corresponding to form Z212.

Though the precise identification of the conformers of the E and Z ketenes present in the photolyzed MP matrix shall be considered as tentative (it is probable that several forms are indeed represented, since the energy involved in the photolysis is large enough to allow for different forms to be accessible), we considered E112 and Z212 forms as representative of the E- and Z-type ketene isomers and best candidates for major presence in the matrix. The calculated IR spectra for these two forms are given in Table S2 (Supporting Information). Their predicted νC═C═O ketene antisymmetric stretching bands are compared to the experimental ones in Figure 6. The relative wavenumber position of the bands of the two forms agrees with the expectation that the E-form is produced first. Most probably, this occurs in a similar way as found for ketenes' production during photolysis of matrix-isolated phenol,[55] i.e., from the direct cleavage of the C−CH_2 bond α to the carbonyl of the nonobserved 4-methoxycarbonyl-2,4-cyclohexanedienone intermediate resulting from the *ortho*-recombination of H and MP radicals. The E-type ketene is later on converted into the more stable Z form via photoinduced E−Z isomerization. Note that the irradiation at λ > 234 nm led only to a very small production of the Z ketene form (see Figures 5 and 6)—the main photoproducts of this irradiation are the methylparaben radical and E ketene. On the other hand, the accumulated product after irradiation at λ > 325 nm is the Z ketene form, while the populations of both the radical and E ketene were found to be nearly stationary. It is also interesting to note that the final populations of the E- and Z-type ketene forms (after 14 min of irradiation at λ > 234 nm followed by an additional 2 h of irradiation at λ > 325 nm) are nearly equal (see Figures 5 and 6; note that in Figure 6 the intrinsic intensities of the bands are different in the two forms: 994 and 1671 km mol^{-1}, respectively, for E and Z isomers, as shown in the calculated spectra shown in the bottom panel of the figure). Note also that, in the spectrum obtained at the end of the irradiation program shown in Figure 6, the characteristic band of CO in argon matrix (~2138 cm^{-1})[77−79] was also present. This indicates that, as found for other matrix-isolated ketenes subjected to UV irradiation,[79] extrusion of CO from the ketene forms produced in the present experiments is also taking place to a minor extent.

The fact that the Z-type ketene is the main product resulting from the irradiation at λ > 325 nm was confirmed by observation of several other bands in the spectra obtained after this irradiation (~1697, 1639, 1554/1549, 1314, 1298, 1246, 1195, 1152, 1082, 1027, and 906 cm^{-1}), which match well the most intense predicted infrared bands of Z212 (1695, 1634, 1579, 1309, 1296, 1218, 1185, 1147, 1078, 1015, and 909 cm^{-1}, respectively; see also Table 3 and Table S2, Supporting Information). In the case of the E form, less bands could be observed, in part because many bands of this isomer were expected to occur underneath those of other species. Nevertheless, bands at 1727, 1642, 1594, 1256/1254, 1093, 1073, 1000, and 585 cm^{-1} can be tentatively assigned to this form (the band at 1727 cm^{-1} has a major contribution from the methylparaben radical). These bands have theoretically predicted counterparts for E112 at 1716, 1640, 1598, 1234, 1086, 1064, 925, and 597 cm^{-1} (see Table 3 and also Table S2, Supporting Information).

Figure 8 summarizes the results of the photochemical experiments: upon irradiation at λ > 234 nm, methylparaben

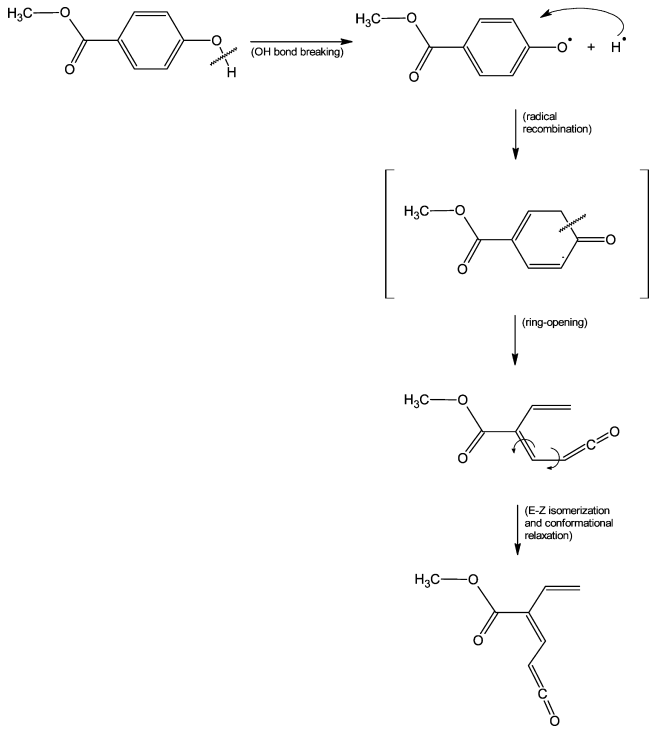

Figure 8. UV-induced reactions observed upon irradiation (λ > 234 nm, 14 min + λ > 325 nm, 2 h) of matrix-isolated methylparaben. The intermediate under brackets was not observed; it is postulated on the basis of previous observations on the photochemistry of phenol and phenol-d_5.[55]

undergoes cleavage of the O−H bond, forming the MP radical plus H atom; recombination of the radicals within the matrix cage shall lead to the nonobserved 4-methoxycarbonyl-2,4-cyclohexanedienone intermediate which quickly undergoes a ring-opening photoreaction leading to formation of the E ketene isomer of methylparaben. The E-type ketene is later on

dx.doi.org/10.1021/jp408366x | J. Phys. Chem. B 2013, 117, 13543−13555

converted into the more stable Z form via photoinduced E−Z isomerization, favored upon irradiation at $\lambda > 325$ nm.

4. CONCLUSIONS

Methylparaben was isolated in solid argon and characterized structurally by a combined infrared spectroscopy/quantum chemistry approach. The analysis of the potential energy surface of the molecule reveals the existence of two almost isoenergetic (ΔE^0 = 0.37 kJ mol^{-1}) *s-cis* carboxylic ester low-energy conformers and two high-energy (ΔE^0 = ∼50 kJ mol^{-1}) *s-trans* carboxylic ester conformers of MP. In spite of the two lower-energy *s-cis* forms being predicted to exist in the room temperature vapor of the compound, upon isolation of MP in an argon matrix (15 K), only the lowest energy conformer was found to subsist, due to occurrence of extensive conformational cooling during matrix deposition. The infrared spectrum of this conformer was obtained and interpreted.

Since harmful effects on human skin exposed to the sunlight have been demonstrated,[16−18] the chemical processes resulting from *in situ* irradiation of the matrix-isolated MP with a broadband UV source were also investigated. These studies revealed extensive photoconversion of MP into highly reactive methylparaben radical and isomeric ketenes, supporting the recent concerns regarding uses of MP, in particular when the compound has to be exposed to UV light. Specifically, the observed photochemistry of matrix-isolated MP was found to follow closely that previously observed for phenol in solid argon:[55] upon irradiation at $\lambda > 234$ nm, methylparaben undergoes cleavage of the O−H bond, forming the MP radical plus H atom; recombination of the radicals leads most probably to the nonobserved 4-methoxycarbonyl-2,4-cyclohexanedienone intermediate, which quickly undergoes a ring-opening photoreaction leading to formation of the E ketene isomeric of methylparaben. The E-type ketene then converts into the more stable Z ketene form via photoinduced E−Z isomerization, favored upon irradiation at $\lambda > 325$ nm.

■ ASSOCIATED CONTENT

Supporting Information

Table S1, with the definition of the symmetry coordinates used in the normal coordinate analyses of methylparaben; Table S2, with B3LYP/6-311++G(d,p) calculated infrared spectra for methylparaben radical and ketenes E112 and Z212; Table S3, with energies and relative energies of the ketene isomeric forms of methylparaben. Figure S1, with the B3LYP/6-311++G(d,p) calculated potential energy profiles for internal rotation about the exocyclic C−C and C−O bonds in methylparaben (III → IV conversion through rotation of the methoxycarbonyl and hydroxyl fragments); Figure S2, with the B3LYP/6-311++G(d,p) calculated potential energy profiles for internal rotation about the $C_{(11)}$−$O_{(13)}$ bond in methylparaben, corresponding to the I−III and II−IV interconversions; Figure S3, with the B3LYP/6-311++G(d,p) calculated potential energy profiles for methyl internal rotation in methylparaben conformers; Figure S4, with the near-IR spectrum (7400−6800 cm^{-1} spectral range) of methylparaben in an argon matrix (15 K); Figure S5, with the previously observed[55] photochemistry of matrix-isolated phenol. This material is available free of charge via the Internet at http://pubs.acs.org.

■ AUTHOR INFORMATION

Corresponding Author

*E-mail: rfausto@ci.uc.pt.

Notes

The authors declare no competing financial interest.

■ ACKNOWLEDGMENTS

These studies were performed under project PTDC/QUI-QUI/111879/2009 (also funded by COMPETE-QREN-EU). N.K. acknowledges the Portuguese Science Foundation (Fundação para a Ciência e a Tecnologia; FCT) for her postdoctoral research grant (SFRH/BPD/88372/2012).

■ REFERENCES

(1) Soni, M. G.; Taylor, S. L.; Greenberg, N. A.; Burdock, G. A. Evaluation of the Health Aspects of Methylparaben: a Review of the Published Literature. *Food Chem. Toxicol.* **2002**, *40*, 1335−1373.

(2) Decker, R. L.; Wenninger, J. A. Frequency of Preservative Use in Cosmetic Formulas as Disclosed to FDA − 1987. *Cosmet. Toiletries* **1987**, *102*, 21−24.

(3) Soni, M. G.; Burdock, G. A.; Taylor, S. L.; Greenberg, N. A. Safety Assessment of Propyl Paraben: a Review of the Published Literature. *Food Chem. Toxicol.* **2001**, *39*, 513−532.

(4) Zhang, Q.; Lian, M. L.; Liu, J.; Cui, H. High-Performance Liquid Chromatographic Assay of Parabens in Wash-off Cosmetic Products and Foods Using Chemiluminescence Detection. *Anal. Chim. Acta* **2005**, *537*, 31−39.

(5) Cantwell, F. F. Re-column Reactions to Eliminate Interferents in the Liquid Chromato-graphic Analysis of p-Hydroxybenzoates in Complex Pharmaceuticals. *Anal. Chem.* **1976**, *48*, 1854−1859.

(6) Soni, M. G.; Carabin, I. G.; Burdock, G. A. Safety Assessment of Esters of p-Hydroxybenzoic Acid (Parabens). *Food Chem. Toxicol.* **2005**, *43*, 985−1015.

(7) Angelini, G.; Bucci, R.; Colosimo, M.; Margonelli, A. Stability of Methyl p-Hydroxybenzoate (Methylparaben) to Gamma Radiolysis. *Radiat. Phys. Chem.* **1998**, *51*, 77−83.

(8) Rodrigues, C.; Lok, E.; Nera, E.; Iverson, F.; Page, D.; Karpinski, K.; Clayson, D. B. Short-term Effects of Various Phenols and Acids on the Fischer 344 Male Rat Forestomach Rpithelium. *Toxicology* **1986**, *38*, 103−117.

(9) Matthews, C.; Davidson, J.; Bauer, E.; Morrison, J. L.; Richardson, A. P. p-Hydroxybenzoic Acid Esters as Preservatives. II. Acute and Chronic Toxicity in Dogs, Rats, and Mice. *J. Am. Pharm. Assoc.* **1956**, *45*, 260−267.

(10) Kawachi, T.; Yahagi, T.; Kada, T.; Tazima, Y.; Ishidate, M.; Sasaki, M.; Sugiyama, T. Cooperative Programme on Short-Term Assays for Carcinogenicity in Japan. *IARC Sci. Publ.* **1980**, 323−330.

(11) Oh, S. Y.; Fujii, M.; Takeda, Y.; Yoda, K.; Utoguchi, N.; Matsumoto, M.; Watanabe, Y. The Effect of Ethanol on the Simultaneous Transport and Metabolism of Methyl p-Hydroxybenzoate in Excised Skin of Yucatan Micropig. *Int. J. Pharm.* **2002**, *236*, 35−42.

(12) Cross, S. E.; Roberts, M. S. The Effect of Occlusion on Epidermal Penetration of Parabens from a Commercial Allergy Test Ointment, Acetone and Ethanol Vehicles. *J. Invest. Dermatol.* **2000**, *115*, 914−918.

(13) Savage, H.; Matsui, E. C.; Wood, R. A.; Keet, C. A. Urinary Levels of Triclosan and Parabens are Associated with Aeroallergen and Food Sensitization. *J. Allergy Clin. Immunol.* **2012**, *130*, 453−460.

(14) Darbre, P. D.; Aljarrah, A.; Miller, W. R.; Coldham, N. G.; Sauer, M. J.; Pope, G. S. Concentrations of Parabens in Human Breast Tumours. *J. Appl. Toxicol.* **2004**, *24*, 5−13.

(15) Harvey, P. W.; Everett, D. J. Significance of the Detection of Esters of p-Hydroxybenzoic Acid (Parabens) in Human Breast Tumours. *J. Appl. Toxicol.* **2004**, *24*, 1−4.

(16) Handa, O.; Kokura, S.; Adachi, S.; Takagi, T.; Naito, Y.; Tanigawa, T.; Yoshida, N.; Yoshikawa, T. Methylparaben Potentiates UV-Induced Damage of Skin Keratinocytes. *Toxicology* **2006**, *227*, 62−72.

(17) Mowad, C. M. Allergic Contact Dermatitis Caused by Parabens: 2 Case Reports and a Review. *Am. J. Contact Dermatitis* **2000**, *11*, 53−56.
(18) Okamoto, Y.; Hayashi, T.; Matsunami, S.; Ueda, K.; Kojima, N. Combined Activation of Methylparaben by Light Irradiation and Esterase Metabolism Toward Oxidative DNA Damage. *Chem. Res. Toxicol.* **2008**, *21*, 1594−1599.
(19) Wang, H.; Zhao, G. Study on the THz Spectra of Four Kinds of Nipagin Esters. *Chin. Opt. Lett.* **2011**, *9*, No. S10503-1.
(20) Mincea, M. M.; Lupsa, I. R.; Cinghita, D. F.; Radovani, C. V.; Talpos, I.; Ostafe, V. Determination of Methylparaben from Cosmetic Products by Ultra Performance Liquid Chromatography. *J. Serb. Chem. Soc.* **2009**, *74*, 669−676.
(21) Claver, J. B.; Valencia, M. C.; Capitán-Vallvey, L. F. Analysis of Parabens in Cosmetics by Low Pressure Liquid Chromatography with Monolithic Column and Chemiluminescent Detection. *Talanta* **2009**, *15*, 499−506.
(22) Hájková, R.; Solich, P.; Pospíšilová, M.; Šícha, J. Simultaneous Determination of Methylparaben, Propylparaben, Sodium Diclofenac and its Degradation Product in a Topical Emulgel by Reversed-phase Liquid Chromatography. *Anal. Chim. Acta* **2002**, *467*, 91−96.
(23) Kollmorgen, D.; Kraut, B. Determination of Methylparaben, Propylparaben and Chlorpromazinecin Chlorpromazine Hydrochloride Oral Solution by High-Performance Liquid Chromatography. *J. Chromatogr., B* **1998**, *707*, 181−187.
(24) Han, Y.; Jia, X.; Liu, X.; Duan, T.; Chen, H. DLLME Combined with GC−MS for the Determination of Methylparaben, Ethylparaben, Propylparaben and Butylparaben in Beverage Samples. *Chromatographia* **2010**, *72*, 351−355.
(25) Ferreira, A. M. C.; Möder, M.; Laespada, M. E. F. GC-MS Determination of Parabens, Triclosan and Methyl Triclosan in Water by in situ Derivatisation and Stir-Barsorptive Extraction. *Anal. Bioanal. Chem.* **2011**, *399*, 945−953.
(26) Kang, S. H.; Kim, H. Simultaneous Determination of Methylparaben, Propylparaben and Thimerosal by High-Performance Liquid Chromatography and Electrochemical Detection. *J. Pharm. Biomed. Anal.* **1997**, *15*, 1359−1364.
(27) Gomes, P. C. F. L.; Barnes, B. B.; Santos-Neto, A. J.; Lancas, F. M.; Snow, N. H. Determination of Steroids, Caffeine and Methylparaben in Water Using Solid Phase Microextraction-Comprehensive Two Dimensional Gas Chromatography − Time of Flight Mass Spectrometry. *J. Chromatogr., A* **2013**, *1299*, 126−130.
(28) Chocholous, P.; Satínsky, D.; Solich, P. Fast Simultaneous Spectrophotometric Determination of Naphazoline Nitrate and Methylparaben by Sequential Injection Chromatography. *Talanta* **2006**, *70*, 408−413.
(29) Kannathasan, K.; Senthilkumar, A.; Venkatesalu, V. Mosquito Larvicidal Activity of Methyl p-Hydroxybenzoate Isolated from the Leaves of Vitex trifolia Linn. *Acta Trop.* **2011**, *115*, 115−118.
(30) Guadarrama, P.; Fomine, S.; Salcedo, R.; Martínez, A. Construction of Simplified Models to Simulate Estrogenic Disruptions by Esters of 4-Hydroxy Benzoic Acid (Parabens). *Biophys. Chem.* **2008**, *137*, 1−6.
(31) Naik, K. M.; Nandibewoor, S. T. Spectral Characterization of the Binding and Conformational Changes of Bovine Serum Albumin upon Interaction with an Anti-fungal Drug, Methylparaben. *Spectrochim. Acta, Part A* **2013**, *105*, 418−423.
(32) Sajan, D.; Joe, H.; Jayakumar, V. S.; Zaleski, J. Structural and Electronic Contributions to Hyperpolarizability in Methyl p-Hydroxybenzoate. *J. Mol. Struct.* **2006**, *785*, 43−53.
(33) Dhanuskodi, S.; Manikandan, S. Spectral Studies of Methyl p-Hydroxybenzoate: an Organic Non-linear Optical Crystalline Material. *Cryst. Res. Technol.* **2004**, *39*, 586−591.
(34) Gelbrich, T.; Braun, D. E.; Ellern, A.; Griesser, U. J. Four Polymorphs of Methylparaben: Structural Relationships and Relative Energy Differences. *Cryst. Growth Des.* **2013**, *13*, 1206−1217.
(35) Lindpaintner, E. Mikroskopische Untersuchungen an Polymorphen Substanzen. *Mikrochemie* **1939**, *27*, 21−41.
(36) Vijayan, N.; Bhagavannarayana, G.; Gopalakrishnan, R.; Ramasamy, P. Structural and Optical Characterization on Solution Grown Methyl p-Hydroxybenzoate Single Crystals. *Indian J. Chem., Sect. A* **2007**, *46*, 70−73.
(37) Aithal, P. S.; Rao, M. Novel Nonlinear Optical Crystal of Methyl p-Hydroxybenzoate. *J. Cryst. Growth* **1995**, *153*, 60−62.
(38) Nath, N. K.; Aggarwal, H.; Nangia, A. Crystal Structure of Methylparaben Polymorph II. *Cryst. Growth Des.* **2011**, *11*, 967−971.
(39) Rosado, M. T. S.; Lopes de Jesus, A. J.; Reva, I. D.; Fausto, R.; Redinha, J. S. Conformational Cooling Dynamics in Matrix-Isolated 1,3-butanediol. *J. Phys. Chem. A* **2009**, *113*, 7499−7507.
(40) Borba, A.; Gómez-Zavaglia, A.; Fausto, R. Conformational Cooling and Conformationally Selective Aggregation in Dimethyl Sulfite Isolated in Solid Rare Gases. *J. Mol. Struct.* **2006**, *794*, 196−203.
(41) Reva, I. D.; Lopes de Jesus, A. J.; Rosado, M. T. S.; Fausto, R.; Eusébio, M. E.; Redinha, J. S. Stepwise Conformational Cooling Towards a Single Isomeric State in the Four Internal Rotors System 1,2-Butanediol. *Phys. Chem. Chem. Phys.* **2006**, *8*, 5339−5349.
(42) Reva, I. D.; Stepanian, S. G.; Adamowicz, L.; Fausto, R. Missing Conformers: Comparative Study of Conformational Cooling in Cyanoacetic Acid and Methyl Cyanoacetate Isolated in Low Temperature Inert Gas Matrixes. *Chem. Phys. Lett.* **2003**, *374*, 631−638.
(43) Frisch, M. J.; Trucks, G. W.; Schlegel, H. B.; Scuseria, G. E.; Robb, M. A.; Cheeseman, J. R.; Montgomery, J. A., Jr.; Vreven, T.; Kudin, K. N.; Burant, J. C.; Millam, J. M.; Iyengar, S. S.; Tomasi, J.; Barone, V.; Mennucci, B.; Cossi, M.; Scalmani, G.; Rega, N.; Petersson, G. A.; Nakatsuji, H.; Hada, M.; Ehara, M.; Toyota, K.; Fukuda, R.; Hasegawa, J.; Ishida, M.; Nakajima, T.; Honda, Y.; Kitao, O.; Nakai, H.; Klene, M.; Li, X.; Knox, J. E.; Hratchian, H. P.; Cross, J. B.; Bakken, V.; Adamo, C.; Jaramillo, J.; Gomperts, R.; Stratmann, R. E.; Yazyev, O.; Austin, A. J.; Cammi, R.; Pomelli, C.; Ochterski, J. W.; Ayala, P. Y.; Morokuma, K.; Voth, G. A.; Salvador, P.; Dannenberg, J. J.; Zakrzewski, V. G.; Dapprich, S.; Daniels, A. D.; Strain, M. C.; Farkas, O.; Malick, D. K.; Rabuck, A. D.; Raghavachari, K.; Foresman, J. B.; Ortiz, J. V.; Cui, Q.; Baboul, A. G.; Clifford, S.; Cioslowski, J.; Stefanov, B. B.; Liu, G.; Liashenko, A.; Piskorz, P.; Komaromi, I.; Martin, R. L.; Fox, D. J.; Keith, T.; Al-Laham, M. A.; Peng, C. Y.; Nanayakkara, A.; Challacombe, M.; Gill, P. M. W.; Johnson, B.; Chen, W.; Wong, M. W.; Gonzalez, C.; Pople, J. A. *Gaussian 03*, revision C.02; Gaussian, Inc.: Wallingford, CT, 2004.
(44) Becke, A. D. Density-Functional Exchange-Energy Approximation with Correct Asymptotic Behavior. *Phys. Rev. A* **1988**, *38*, 3098−3100.
(45) Lee, C. T.; Yang, W. T.; Parr, R. G. Development of the Colle-Salvetti Correlation-Energy Formula into a Functional of the Electron Density. *Phys. Rev. B* **1988**, *37*, 785−789.
(46) McLean, A. D.; Chandler, G. S. Contracted Gaussian Basis Sets for Molecular Calculations. I. Second Row Atoms, Z=11−18. *J. Chem. Phys.* **1980**, *72*, 5639−5648.
(47) Schachtschneider, J. H.; Mortimer, F. S. Vibrational Analysis of Polyatomic Molecules. VI. FORTRAN IV Programs for Solving the Vibrational Secular Equation and for the Least-Squares Refinement of Force Constants. Project No. 31450. Structural Interpretation of Spectra; Shell Development Co., 1969.
(48) Pulay, P.; Fogarasi, G.; Pang, F.; Boggs, J. E. Systematic Ab Initio Gradient Calculation of Molecular Geometries, Force Constants, and Dipole Moment Derivatives. *J. Am. Chem. Soc.* **1979**, *101*, 2550−2560.
(49) Berden, G.; Meerts, W. L.; Schmitt, M.; Kleinermanns, K. High Resolution UV Spectroscopy of Phenol and the Hydrogen Bonded Phenol-Water Cluster. *J. Chem. Phys.* **1996**, *104*, 972−982.
(50) Senent, M. L.; Villa, M.; Meléndez, F. J.; Domínguez-Gómez, R. Ab Initio Study of the Rotational-Torsional Spectrum of Methyl Formate. *Astrophys. J.* **2005**, *627*, 567−576.
(51) Senent, M. L.; Domínguez-Gómez, R.; Carvajal, M.; Kleiner, I. Highly Correlated Ab Initio Study of the Far Infrared Spectra of Methyl Acetate. *J. Chem. Phys.* **2013**, *138*, No. 044319.

(52) Curl, R. F., Jr. Microwave Spectrum, Barrier to Internal Rotation, and Structure of Methyl Formate. *J. Chem. Phys.* **1959**, *30*, 1529−1536.
(53) Teixeira-Dias, J. J. C.; Fausto, R. A Molecular Mechanics Force Field for Conformational Analysis of Simple Acyl Chlorides, Carboxylic Acids and Esters. *J. Mol. Struct.* **1986**, *144*, 199−213.
(54) Tudorie, M.; Kleiner, I.; Hougen, J. T.; Melandri, S.; Sutikdja, L. W.; Stahl, W. A Fitting Program for Molecules with Two Inequivalent Methyl Tops and a Plane of Symmetry at Equilibrium: Application to New Microwave and Millimeter-Wave Measurements of Methyl Acetate. *J. Mol. Spectrosc.* **2011**, *269*, 211−225.
(55) Giuliano, B. M.; Reva, I.; Lapinski, L.; Fausto, R. Infrared Spectra and Ultraviolet-Tunable Laser Induced Photochemistry of Matrix-Isolated Phenol and Phenol-d_5. *J. Chem. Phys.* **2012**, *136*, No. 024505.
(56) Maçôas, E. M. S.; Fausto, R.; Pettersson, M.; Khriachtchev, L.; Räsänen, M. Infrared Induced Rotamerization of Oxalic Acid Monomer in an Argon Matrix. *J. Phys. Chem. A* **2000**, *104*, 6956−6961.
(57) Maçôas, E. M. S.; Kriachtchev, L.; Pettersson, M.; Fausto, R.; Räsänen, M. Rotational Isomerism in Acetic Acid: The First Experimental Observation of the High-Energy Conformer. *J. Am. Chem. Soc.* **2003**, *125*, 16188−16189.
(58) Lapinski, L.; Reva, I.; Rostkowska, H.; Halasa, A.; Fausto, R.; Nowak, M. J. Conformational Transformation in Squaric Acid Induced by Near-IR Laser Light. *J. Phys. Chem. A* **2013**, *117*, 5251−5259.
(59) Reva, I.; Nowak, M. J.; Lapinski, L.; Fausto, R. Spontaneous Tunneling and Near-Infrared-Induced Interconversion Between the Amino-Hydroxy Conformers of Cytosine. *J. Chem. Phys.* **2013**, *136*, No. 064511.
(60) Sharma, A.; Reva, I.; Fausto, R. Conformational Switching Induced by Near-Infrared Laser Irradiation. *J. Am. Chem. Soc.* **2009**, *131*, 8752−8753.
(61) Bazsó, G.; Magyarfalvi, G.; Tarczay, G. Tunneling Lifetime of the ttc/VIp Conformer of Glycine in Low-Temperature Matrices. *J. Phys. Chem. A* **2012**, *116*, 10539−10547.
(62) Bazsó, G.; Najbauer, E. E.; Magyarfalvi, G.; Tarczay, G. Near-Infrared Laser Induced Conformational Change of Alanine in Low-Temperature Matrixes and the Tunneling Lifetime of its Conformer VI. *J. Phys. Chem. A* **2013**, *117*, 1952−1962.
(63) Nunes, C. M.; Lapinski, L.; Fausto, R.; Reva, I. Near-IR Laser Generation of a High-Energy Conformer of L-alanine and the Mechanism of its Decay in a Low-Temperature Nitrogen Matrix. *J. Chem. Phys.* **2013**, *138*, No. 125101.
(64) Lopes, S.; Domanskaya, A. V.; Fausto, R.; Räsänen, M.; Khriachtchev, L. Formic and Acetic Acids in a Nitrogen Matrix: Enhanced Stability of the Higher-Energy Conformer. *J. Chem. Phys.* **2010**, *133*, No. 144507.
(65) Lam, S.-M.; Sin, J.-C.; Abdullah, A. Z.; Mohamed, A. R. Green Hydrothermal Synthesis of ZnO Nanotubes for Photocatalytic Degradation of Methylparaben. *Mater. Lett.* **2013**, *93*, 423−426.
(66) Tsourounaki, K.; Aroniada, G.; Psillakis, E. Photodegradation of Methylparaben in Various Environmental Aqueous Solutions by 254 nm Irradiation. *Proc. 3rd. Intl. Conf. on Industrial and Hazardous Waste Management* **2012**, 1−7.
(67) Sánchez-Martín, J.; Beltrán-Heredia, J.; Domínguez, J. R. Advanced Photochemical Degradation of Emerging Pollutants: Methylparaben. *Water, Air, Soil Pollut.* **2013**, *224*, 1483−1495.
(68) Lin, Y.; Ferronato, C.; Deng, N.; Wu, F.; Chovelon, J.-M. Photocatalytic Degradation of Methylparaben by TiO2: Multivariable Experimental Design and Mechanism. *Appl. Catal., B* **2009**, *88*, 32−41.
(69) Loh, W.; Beezer, A. E.; Mitchell, J. C. Thermochemical Investigation of Possible Interactions Between Urea and Some Sparingly Soluble Solutes in Aqueous Solution. *Thermochim. Acta* **1995**, *255*, 83−91.
(70) Kuş, N.; Breda, S.; Reva, I.; Tasal, E.; Ogretir, C.; Fausto, R. FTIR Spectroscopic and Theoretical Study of the Photochemistry of Matrix-Isolated Coumarin. *Photochem. Photobiol.* **2007**, *83*, 1237−1253, 1541−1542.
(71) Breda, S.; Reva, I.; Lapinski, L.; Fausto, R. Photochemical α-Cleavage in Pyran-2-thione: Generation of Aldehyde-Thioketene and Thioaldehyde-Ketene Photoproducts. *ChemPhysChem* **2005**, *6*, 602−604.
(72) Reva, I. D.; Breda, S.; Roseiro, T.; Eusébio, E.; Fausto, R. On the Pyrolysis Mechanism of 2-Pyranones and 2-Pyranthiones: Thermally Induced Ground Electronic State Chemistry of Pyran-2-thione. *J. Org. Chem.* **2005**, *70*, 7701−7710.
(73) Kuş, N.; Reva, I.; Bayari, S.; Fausto, R. In Situ Photoproduction of Dichlorodibenzo-p-Dioxin from Non-Ionic Triclosan Isolated in Solid Argon. *J. Mol. Struct.* **2012**, *1007*, 88−94.
(74) *GaussView*, version 3.0; Gaussian, Inc.: Pittsburgh, PA (2002−2003 Semichem, Inc).
(75) Baldwin, J. E.; Krueger, S. M. Stereoselective Photochemical Electrocyclic Valence Isomerizations of α-Phellandrene Conformational Isomers. *J. Am. Chem. Soc.* **1969**, *91*, 6444−6447.
(76) Marzec, K. M.; Reva, I.; Fausto, R.; Proniewicz, L. M. Comparative Matrix Isolation Infrared Spectroscopy Study of 1,3- and 1,4-Diene Terpinenes (γ-Terpinene and α-Phellandrene). *J. Phys. Chem. A* **2011**, *115*, 4342−4353.
(77) Dubost, H.; Abouaf-Marguin, L. Infrared-Spectra of Carbon-Monoxide Trapped in Solid Argon. Double-Doping Experiments with H_2O, NH_3 and N_2. *Chem. Phys. Lett.* **1972**, *17*, 269−273.
(78) Lopes, S.; Gómez-Zavaglia, A.; Lapinski, L.; Fausto, R. Conformational Flexibility, UV-Induced Decarbonylation, and FTIR spectra of 1-Phenyl-1,2-Propanedione in Solid Xenon and in the Low Temperature Amorphous Phase. *J. Phys. Chem. A* **2005**, *109*, 5560−5570.
(79) Krupa, J.; Olbert-Majkut, A.; Reva, I.; Fausto, R.; Wierzejewska, M. Ultraviolet-Tunable Laser Induced Phototransformations of Matrix Isolated Isoeugenol and Eugenol. *J. Phys. Chem. B* **2012**, *116*, 11148−11158.